

Cells satisfy the mitotic checkpoint in Taxol, and do so faster in concentrations that stabilize syntelic attachments

Zhenye Yang,¹ Alison E. Kenny,¹ Daniela A. Brito,² and Conly L. Rieder^{1,2,3}

¹Division of Translational Medicine, Wadsworth Center, NY State Department of Health, Albany, NY 12201

²Department of Biomedical Sciences, School of Public Health, State University of New York at Albany, Albany, NY 12201

³Marine Biology Laboratory, Woods Hole, MA 02543

To determine why the duration of mitosis (DM) is less in Taxol than in nocodazole or Eg5 inhibitors we studied the relationship between Taxol concentration, the DM, and the mitotic checkpoint. We found that unlike for other spindle poisons, in Taxol the DM becomes progressively shorter as the concentration surpasses $\sim 0.5 \mu\text{M}$. Studies on RPE1 and PtK2 expressing GFP/cyclin B or YFP/Mad2 revealed that cells ultimately satisfy the checkpoint in Taxol and do so faster at concentrations $>0.5 \mu\text{M}$. Inhibiting the aurora-B kinase in Taxol-treated

RPE1 cells accelerates checkpoint satisfaction by stabilizing syntelic kinetochore attachments and reduces the DM to ~ 1.5 h regardless of drug concentration. A similar stabilization of syntelic attachments by Taxol itself appears responsible for accelerated checkpoint satisfaction at concentrations $>0.5 \mu\text{M}$. Our results provide a novel conceptual framework for how Taxol prolongs mitosis and caution against using it in checkpoint studies. They also offer an explanation for why some cells are more sensitive to lower versus higher Taxol concentrations.

Introduction

During cell division the mitotic checkpoint minimizes aneuploidy by delaying anaphase and exit from mitosis until all kinetochores are stably attached to microtubules (MTs). When the checkpoint cannot be satisfied, i.e., in the presence of one or more unattached kinetochores, many human cells escape mitosis after a prolonged (~ 20 h) delay to form tetraploid G1 cells. During this process, termed mitotic slippage, the cyclin B subunit of the cyclin B/CDK1 kinase is slowly destroyed in an APC-dependent manner in the presence of an active checkpoint. As a result, over time cyclin B/CDK1 activity falls below that needed to maintain the mitotic state (Brito and Rieder, 2006).

Taxol is a MT-stabilizing drug currently used to treat various cancers. Although its mode of action is unknown, entry into mitosis is required for Taxol sensitivity (Sudo et al., 2004) where it is thought to induce apoptosis by inhibiting mitotic checkpoint satisfaction. Yet, when cultured human cells are treated with clinically relevant Taxol concentrations (5–10 nM) mitosis is not arrested. Rather, after a few hours the cells satisfy

the checkpoint and complete division to produce 2–3 daughters (Ikui et al., 2005), many of which (depending on the cell type) die in G1 (Brito and Rieder, 2009). However, at concentrations between 50 and 100 nM, Taxol is widely reported to arrest cells in mitosis until they die or escape via mitotic slippage (Gascoigne and Taylor 2008; Shi et al., 2008).

We recently found that when mitotic checkpoint satisfaction is prevented with nocodazole or Eg5 motor protein inhibitors, human telomerase-immortalized RPE1 cells average ~ 20 h in mitosis before slipping into G1. At the same time, however, we noted that in 500 nM Taxol RPE1 averaged just 12 h in mitosis, and this shortened duration of mitosis (DM) could not be attributed to MT assembly, which occurs also in Eg5 inhibitors. We therefore hypothesized that RPE1 cells ultimately satisfy the checkpoint in 500 nM Taxol as they do in 5 nM Taxol (Brito et al., 2008). To explore this issue further we conducted live cell studies to determine the relationship between Taxol concentration, the DM, and the mitotic checkpoint.

Correspondence to Conly L. Rieder: rieder@wadsworth.org

Abbreviations used in this paper: ACA, anti-centromere antibody; DM, duration of mitosis; MT, microtubule; NEB, nuclear envelope breakdown.

© 2009 Yang et al. This article is distributed under the terms of an Attribution–Noncommercial–Share Alike–No Mirror Sites license for the first six months after the publication date [see <http://www.jcb.org/misc/terms.shtml>]. After six months it is available under a Creative Commons License [Attribution–Noncommercial–Share Alike 3.0 Unported license, as described at <http://creativecommons.org/licenses/by-nc-sa/3.0/>].

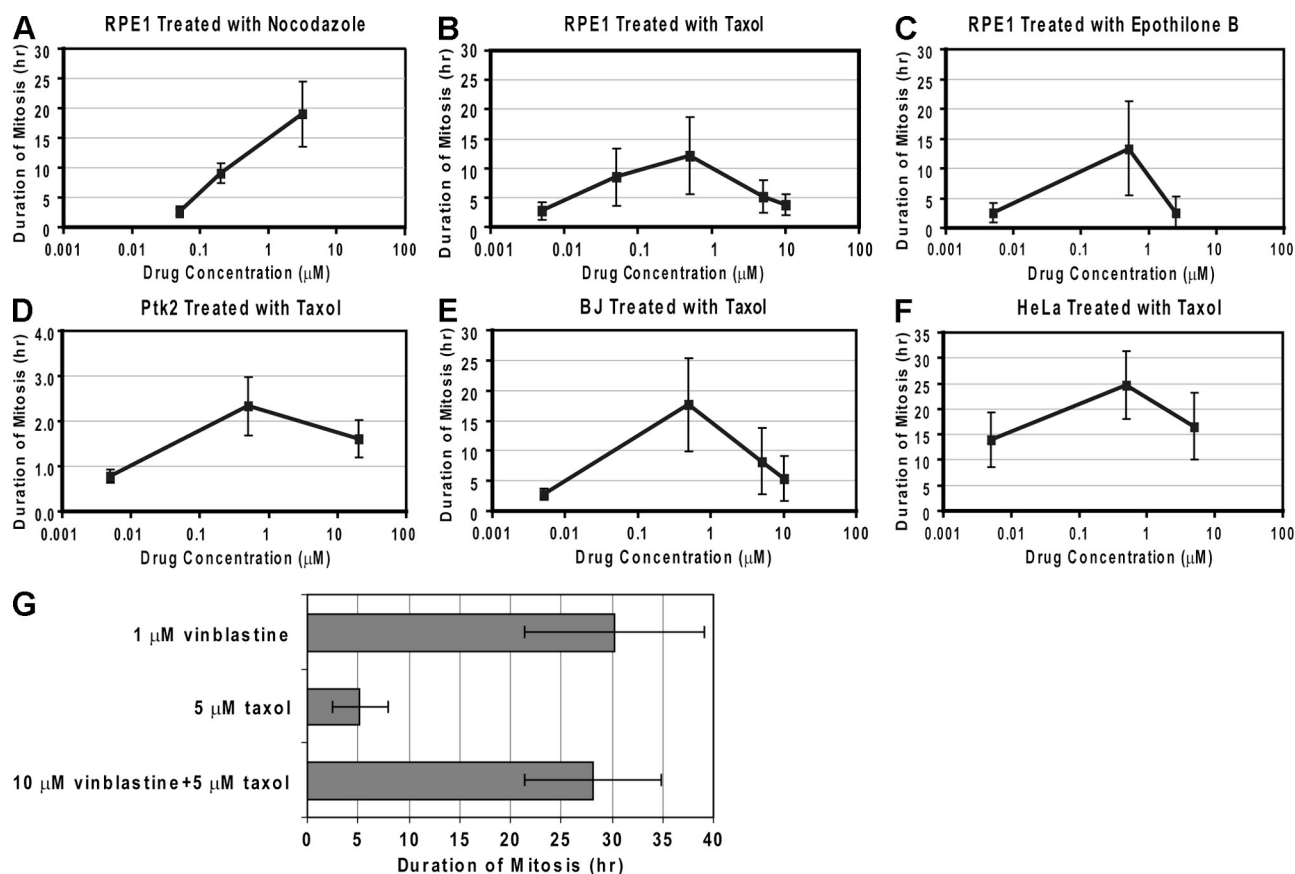


Figure 1. **The duration of mitosis increases with Taxol concentration until a point after which it decreases.** (A–F) Duration of mitosis vs. drug concentration for RPE1 cells treated with nocodazole, Taxol, or Etoposide B, and for Ptk2, human BJ fibroblasts, and HeLa cells treated with Taxol. (G) 5 μM Taxol does not shorten mitosis in RPE1 if microtubule assembly is first prevented by vinblastine.

Results and discussion

For drugs that prevent MT assembly or centrosome separation the DM increases with concentration to a point after which it no longer changes. For HeLa this point ranges from 6 nM in vinblastine to 100 nM in nocodazole (Jordan et al., 1992), and 1.5 μM in *S*-Trityl-L-cysteine (an Eg5 inhibitor; Skoufias et al., 2006). Here, we report that this relationship does not exist for Taxol and its analogues: although the DM in RPE1 cells treated with 5, 50, or 500 nM Taxol increased from 2.5 h to 12 h, in 5 and 10 μM Taxol mitosis averaged, respectively, just 5 and 3.5 h and 99% of the cells survived (Fig. 1 B; Table S1). The same was true for the Taxol analogue etoposide B (Fig. 1 C). This hitherto unreported response to Taxol was also seen in normal human BJ fibroblasts and rat kangaroo kidney (Ptk2) cells, and to a lesser extent in HeLa and U2OS (Fig. 1, D–F; Table S1). Thus, unlike drugs that inhibit MT assembly or centrosome separation, the dose–response curve for the DM in drugs that promote MT stability is biphasic, increasing to a point after which it decreases.

Accelerated exit from mitosis in Taxol concentrations >0.5 μM is due to a drug effect on spindle microtubules

Why is the DM in 5 μM Taxol less than in 0.5 μM Taxol? One idea is that at high concentrations Taxol and etoposide B have

off-site target(s) independent of MTs. To test this we treated RPE1 for 3 h with 3.2 μM nocodazole to prevent MT assembly, and then added 5 μM Taxol. We reasoned that if in the absence of MTs 5 μM Taxol still drives cells from mitosis in \sim 5 h, then there is an off-site target involved. However, even in 3.2 μM nocodazole 5 μM Taxol stimulated MT assembly (unpublished data). We therefore modified this experiment by locking tubulin into paracrystals with 10 μM vinblastine before adding 5 μM Taxol. Under this condition MT formation was inhibited and the cells remained in mitosis for \sim 27 h, similar to after vinblastine treatment alone (Fig. 1 G; Table S1). Thus, the DM is reduced in Taxol concentrations >0.5 μM because of how the drug influences spindle MTs.

Cells satisfy the mitotic checkpoint in Taxol and do so more rapidly at high concentrations

Another idea for why the DM versus concentration plot in Taxol is biphasic is that cells satisfy the checkpoint in Taxol, but do so faster at high concentrations. This is suggested by our data that the DM in 5 nM to 10 μM Taxol is much less than the 20 h seen in cells that cannot satisfy the checkpoint (above). The unchallenged assumption that, as for agents that inhibit MT assembly, Taxol at >100 nM prevents checkpoint satisfaction comes from reports that at these concentrations: (1) spindle assembly is

grossly perturbed, (2) cells are delayed in mitosis, and (3) kinetochores are always present in fixed cells that are positive for the Mad2 checkpoint protein (Waters et al., 1998). However, the checkpoint detects unattached kinetochores, not perturbations in spindle assembly, and it can be satisfied on grossly abnormal spindles (Ikui et al., 2005; Brito et al., 2008). Also, exit from mitosis due to checkpoint satisfaction differs mechanistically from slippage (Brito and Rieder, 2006). Finally, cells lacking Mad2 at kinetochores would rarely be encountered in Taxol-treated cultures because as this condition occurs the cells rapidly exit mitosis.

Mad2 binds to unattached kinetochores (Chen et al., 1996) and is lost from kinetochores as they acquire MTs (Waters et al., 1998; Nicklas et al., 2001). Because checkpoint satisfaction coincides with loss of Mad2 from all kinetochores (Hoffman et al., 2001), we asked if Mad2 is ultimately lost from all kinetochores in Taxol. To answer this we treated RPE1 for 12 h (the average DM in 0.5 μ M Taxol) with 0.5 or 10 μ M Taxol and then added a proteasome inhibitor (10 μ M MG132) 2 h before fixation and Mad2 staining. We reasoned that if in Taxol cells satisfy the checkpoint before exiting mitosis, then preventing exit should enrich for cells lacking Mad2 at all kinetochores. Indeed, although most cells in each concentration exhibited varying degrees of kinetochore-Mad2 staining, cells could be readily located in both in which all kinetochores lacked Mad2 (Fig. S1). These indirect data suggest that cells satisfy the checkpoint in 0.5–10 μ M Taxol before escaping mitosis.

To directly verify this we followed PtK2 stably expressing Mad2/YFP (Mad2/PtK2) as they entered mitosis in 0.5 or 20 μ M Taxol. The DM in these cells, i.e., the period from nuclear envelope breakdown (NEB) to the initiation of cytokinesis, was 45 ± 8 min ($n = 40$), and the period between loss of Mad2/YFP on the last kinetochore and the start of cytokinesis was 17 ± 3 min ($n = 16$). In 0.5 μ M Taxol Mad/PtK2 cells averaged 140 ± 39 min ($n = 92$) in mitosis versus 97 ± 25 min ($n = 54$) in 20 μ M Taxol. We found, in all cases and in both drug concentrations, that Mad2/PtK2 remained in mitosis until the last kinetochore had stably lost its Mad2 signal, ~ 20 min after which an aborted cytokinesis began (Fig. 2, A–C). Also, in both concentrations 85–90% of the kinetochores lost their Mad2 staining within 40 min of NEB, so that the checkpoint was maintained by those few that required longer to become stably depleted of Mad2 (Fig. 2, D–G). From these direct data we conclude that exit from mitosis in Taxol-treated PtK2 cells occurs over a broad (0.5–20 μ M) range of concentrations from checkpoint satisfaction.

Checkpoint satisfaction can also be inferred from a sudden steep drop in cyclin B/GFP fluorescence intensity just before (Chang et al., 2003) or at (Clute and Pines, 1999) chromatid disjunction (Fig. 3, A and D). We therefore followed GFP fluorescence intensity in RPE1 transiently expressing low levels of cyclin B/GFP as they entered mitosis in 0.5 to 10 μ M Taxol. These data were then analyzed to determine if cyclin B/GFP decreased at a “background” level until the cell slipped through mitosis (Brito and Rieder, 2006), or if it slowly decreased as during slippage but then rapidly fell just before mitotic exit as for checkpoint satisfaction in 5 nM Taxol (Brito et al., 2008). In all five cells examined in both 5 and 10 μ M Taxol, mitotic exit

occurred shortly after a sudden precipitous drop in cyclin B/GFP fluorescence (Fig. 3, B and D). This result confirms that, as for PtK2, RPE1 exit from mitosis in ≥ 5 μ M Taxol is due to checkpoint satisfaction.

Although our Mad2 data (Fig. S1) suggest that like PtK2, RPE1 also satisfy the checkpoint in 0.5 μ M Taxol, attempts to demonstrate this by cyclin B/GFP degradation gave results difficult to interpret (Fig. 3 D). However, as for other cell types, in a given spindle poison the DM in RPE1 is highly variable: e.g., 744 ± 399 min for 0.5 μ M Taxol and 1218 ± 424 min in dimethylenastron (Brito et al., 2008). Thus, although some cells may slip through mitosis in 0.5 μ M Taxol before checkpoint satisfaction, the significantly reduced average DM in 0.5 μ M Taxol (12 h) compared with when the checkpoint cannot be satisfied (20 h) suggests that most RPE1 satisfy the checkpoint in 0.5 μ M Taxol.

As previously reported for PtK (Waters et al., 1998), we found no tension on centromeres in PtK2 or RPE1 dividing in 0.5–10 μ M Taxol (Fig. S2). However, in 10 μ M Taxol the cells satisfy the mitotic checkpoint in just several hours. Thus, as concluded recently by others (O’Connell et al., 2008; Uchida et al., 2009), production of the checkpoint signal is not due to a lack of tension on the centromere. That is, there is no centromere-based Mad2-independent tension-sensing pathway for maintaining the checkpoint in the absence of tension between sister kinetochores (Skoufias et al., 2001; Ahonen et al., 2005).

In Taxol, checkpoint satisfaction is delayed until all monotelic and syntelic attachments are converted into amphitelic or stable syntelic attachments

The spindle assembly pathway in Taxol differs from that in untreated cells: in the latter, kinetochore attachment occurs over 15–20 min (Fig. 2 A) from a search-and-capture process, dependent on MT dynamics which is facilitated by the motion of chromosomes and asters (Kapoor et al., 2006; Cai et al., 2009). By contrast, as cells enter mitosis in >100 nM Taxol they form many small asters that migrate at NEB to the chromosomes, where they form a large multipolar spindle (Maekawa et al., 1991; Hornick et al., 2008) (Fig. 4 A). Under this condition astral MTs are substantially shorter, their dynamics are depressed, and the chromosomes are immobile. As a result, the rate kinetochores attach to MTs in Taxol is retarded because it is defined by the movement of the asters and not the dynamic behavior of their associated MTs or chromosomes.

As in a normal mitosis, in Taxol many chromosomes become attached to an aster in a monotelic or syntelic fashion (Fig. 4, A, F, and G, arrowheads). In untreated cells, syntelic attachments are corrected by a constitutive mechanism involving chromosomal passenger complexes, composed of aurora B, survivin, borealin, and INCENP, located in the centromere (Ruchaud et al., 2007). The correction of a syntelic attachment leads to the transient production of a monotelic chromosome with an unattached (and thus checkpoint signaling) kinetochore (Tanaka et al., 2002; Pinsky et al., 2006). In cells containing many syntelic chromosomes but MTs with normal dynamics, as on monastrol spindles formed in Eg5 inhibitors (Kapoor

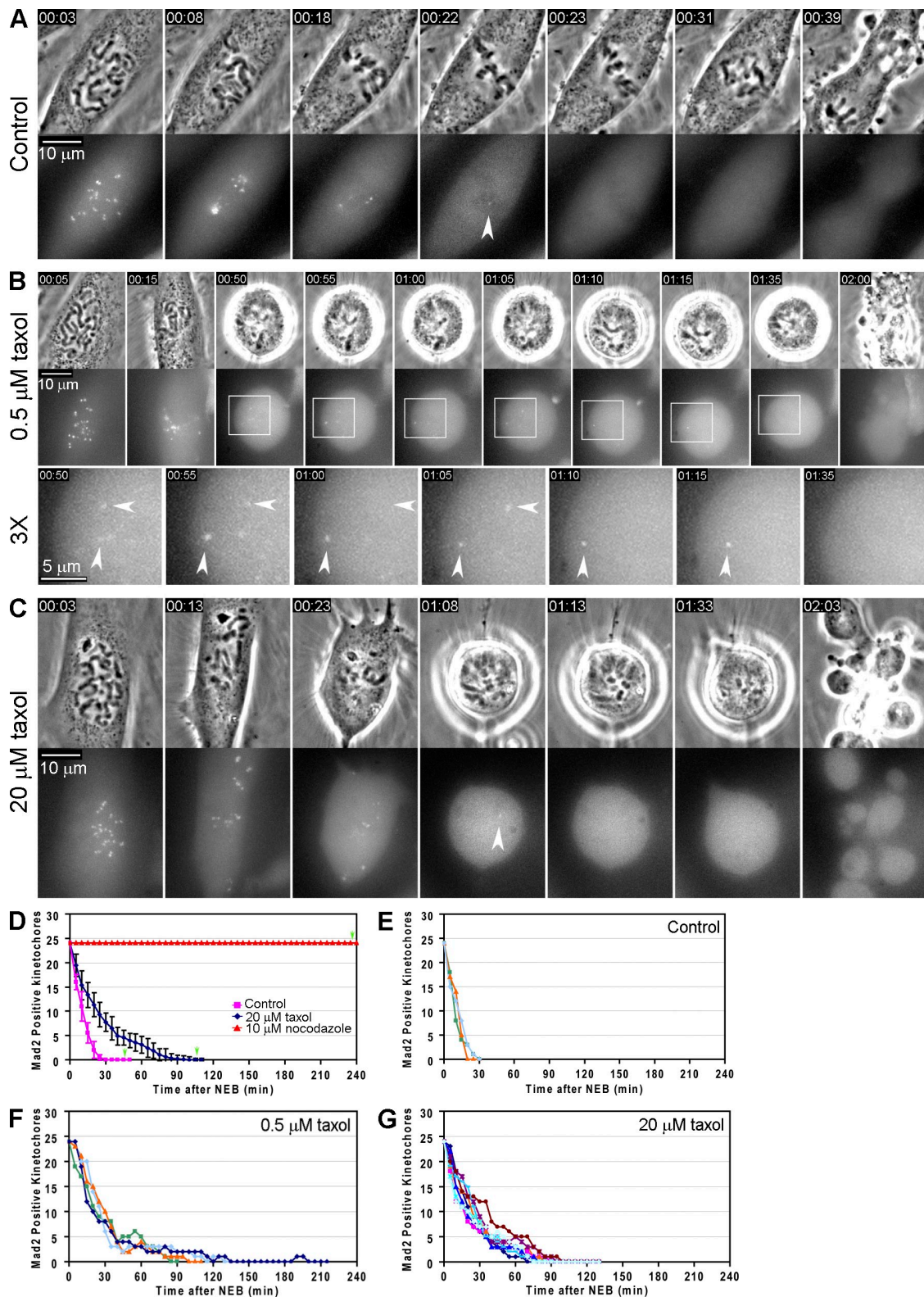


Figure 2. **In Taxol, Mad2 is progressively depleted from kinetochores until the checkpoint is satisfied (see also Fig. S1).** (A–C) YFP/Mad2-Ptk2 cells were followed without treatment (A) or in 0.5 (B) or 20 μM (C) Taxol. Top rows are phase-contrast images and bottom rows are maximum intensity projected YFP fluorescence images of the same cell. Exit from mitosis occurs only after the last Mad2-positive kinetochore (A and C, arrowhead) loses its Mad2. (B) In 0.5 μM Taxol a kinetochore (arrowhead) can lose and then reacquire Mad2, as shown in high-magnification images from the boxed regions. Membrane blebbing is typical as cells exit mitosis in Taxol (C) and is not due to apoptosis. (D) Time vs. average number of Mad2-positive kinetochores in controls and after treatment with 10 μM nocodazole or 20 μM Taxol. (E–G) Similar plots of individual controls (E), or cells treated with 0.5 μM (F) or 20 μM Taxol (G). The number of Mad2-positive kinetochores often transiently increases in 0.5 μM but not 20 μM Taxol.

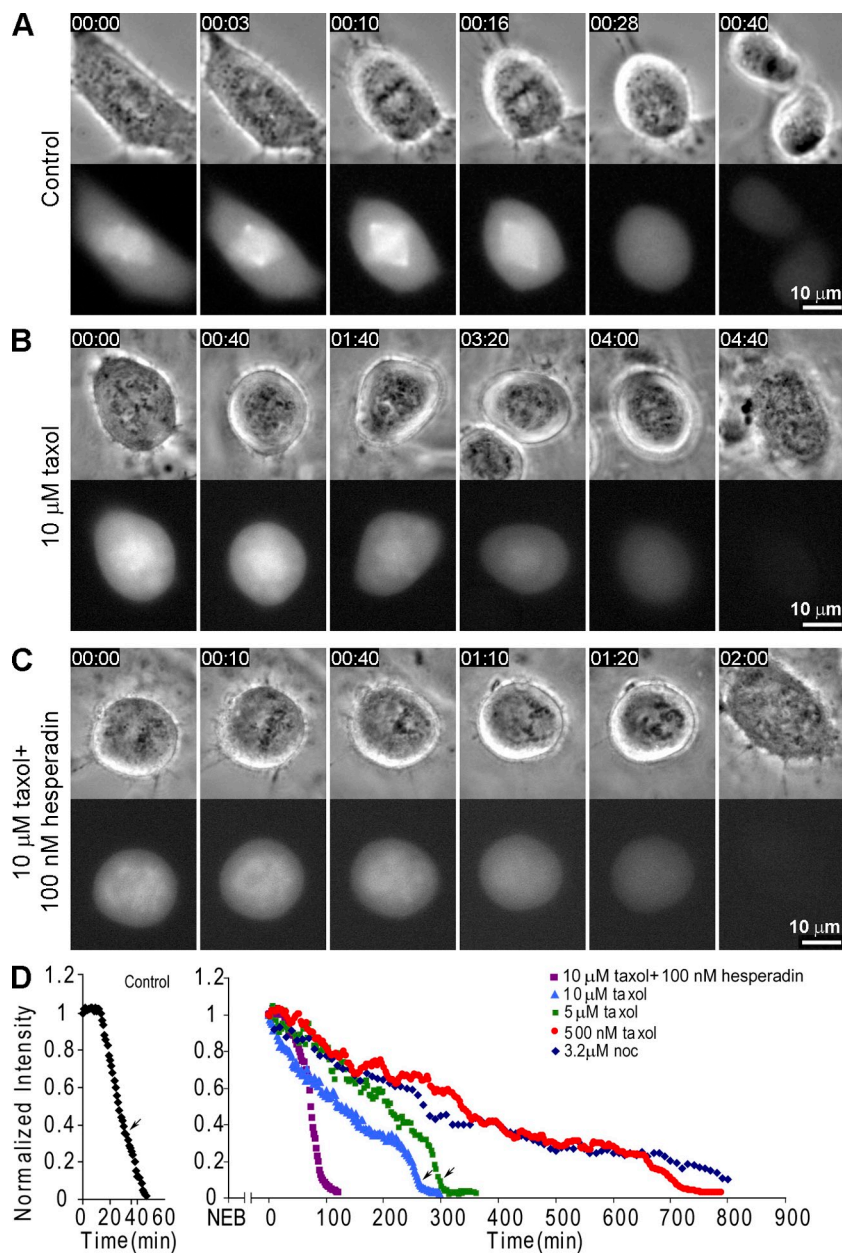


Figure 3. Cyclin B/GFP fluorescence decay increases sharply just before Taxol-treated RPE1 cells exit mitosis. (A) In controls, cyclin B/GFP fluorescence exhibits a sudden, sharp, continuous drop several minutes before chromatid disjunction or cytokinesis (D, arrow), which is clear from the time vs. cyclin B/GFP intensity plot (D). A similar sudden sharp drop in cyclin B/GFP fluorescence is also seen shortly before cells treated with 10 μM Taxol (B) or 10 μM Taxol and 100 nM Hesperadin (C) exit mitosis. (D) Typical normalized cyclin B/GFP fluorescence intensity vs. time plots of controls or cells treated with 3.2 μM nocodazole, 0.5, 5, or 10 μM Taxol, or 10 μM Taxol and Hesperadin. Plots of cyclin B decay in 0.5 μM Taxol were difficult to interpret. Time is in h:min.

et al., 2000), checkpoint satisfaction is prevented because error correction promotes a continuous cycling between syntelic (nonsignaling) and monotelic (signaling) states (Lampson et al., 2004). As a result, killing the correction mechanism in these cells with aurora B inhibitors rapidly stabilizes all syntelic attachments (Hauf et al., 2003; Lampson et al., 2004; Loncarek et al., 2007), which leads to Mad2 depletion at all kinetochores and checkpoint satisfaction (Hauf et al., 2003; Lens et al., 2003).

As in Eg5 inhibitors, the checkpoint cannot be satisfied in Taxol until the asters have gathered all the chromosomes, and then not until all monotelic attachments are converted either into “normal” amphitelic attachments or into syntelic attachments that are somehow stabilized. Although the former process is retarded by the Taxol-induced reduction in aster MT dynamics and inhibition of chromosome motility, the latter is

predicted to be promoted by the stabilizing effects of Taxol on kinetochore MTs.

Stabilizing syntelic attachments in Taxol accelerates exit from mitosis by promoting mitotic checkpoint satisfaction

As on monastrol spindles (above), inhibiting aurora B in Taxol-treated cells accelerates exit from mitosis. We find, in fact, that inhibiting aurora B in RPE1 treated with 0.5 μM Taxol reduces the DM by $\sim 90\%$ (from 12 to 1.5 h; Table S1). An obvious explanation for this is that as in Eg5 inhibitors, inhibiting aurora B in Taxol promotes checkpoint satisfaction by stabilizing syntelic attachments. However, others have concluded that inhibiting aurora B drives cells treated with Taxol or Eg5 inhibitors from mitosis because its activity is required for a functional mitotic checkpoint. Although the supporting data are indirect, the

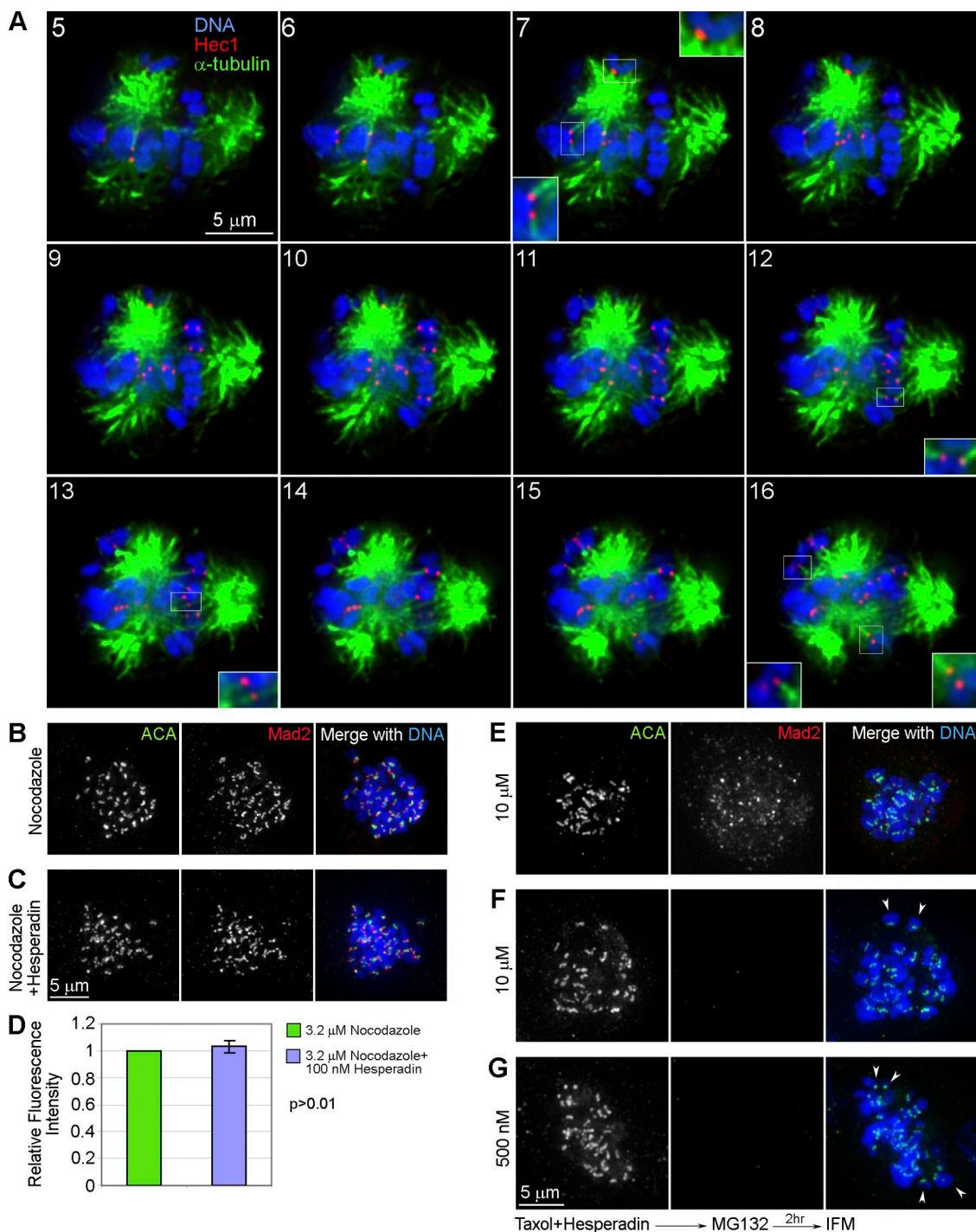


Figure 4. **Chromosomes acquire monotelic, merotelic, or syntelic attachments to asters during spindle assembly in Taxol.** (A) 12 serial sections through a RPE1 cell from a culture treated for 5 h with 0.5 μ M Taxol before fixation and staining for kinetochores (Hec1) and MTs (α -tubulin). Although some kinetochore pairs have acquired amphitelic attachments to adjacent asters (sections 7 and 12, bottom box), others exhibit monotelic (section 16, right-hand box), merotelic (section 13, box), or syntelic (section 7, top box) attachments. (B–D) Inhibiting aurora B does not diminish Mad2 accumulation on kinetochores of nocodazole-treated cells. RPE1 cells were treated for 10 h with 3.2 μ M nocodazole (B) or 3.2 μ M nocodazole and 100 nM Hesperadin (C) before fixation and staining for centromeres (ACA) and Mad2. (D) The kinetochore-Mad2 staining intensity was found by the Student's *t*-test to be the same for both conditions. (E–G) When aurora B is inhibited, Mad2 is progressively depleted from kinetochores in Taxol-treated cells. RPE1 cultures were incubated in Taxol (0.5 μ M or 10 μ M) and Hesperadin for 3–8 h and 10 μ M MG132 was added 2 h before fixation and staining for centromeres and Mad2. Although most cells exhibited variable amounts of kinetochore-Mad2 (E), others could readily be located under both conditions which had no kinetochore-Mad2 staining (F and G). Arrowheads in F and G note clear syntelic chromosomes.

best evidence for this are reports that inhibiting aurora B in nocodazole-treated cells chases them from mitosis prematurely (Ditchfield et al., 2003; Hauf et al., 2003; Vader et al., 2007).

However, one can argue that the nocodazole concentrations used (330–660 nM) were insufficient to completely disrupt MT assembly, and instead promoted the formation of monopolar

spindles containing up to 75% of the normal MT mass (Brinkley et al., 1967; Jordan et al., 1992).

If aurora B activity is required for the mitotic checkpoint, then inhibiting it in cells lacking MTs should induce exit from mitosis in ~30 min, as when bona fide checkpoint components are depleted or inhibited. To test this, we followed RPE1 cells entering mitosis in 3.2 μM nocodazole and a Hesperadin concentration (100 nM) that inhibits aurora B (Hauf et al., 2003). We found that these cells average 17 h in mitosis, similar to the 19 h seen after nocodazole treatment alone (Table S1), and that Mad2 accumulated on kinetochores in these cells to the same level as after nocodazole alone (Fig. 4, B–D). We also found that inhibiting aurora B did not prevent YFP/Mad2 from accumulating on kinetochores in nocodazole-treated PtK2 cells (Fig. 5 B), and when Hesperadin-treated metaphase PtK2 cells lacking Mad2 at most kinetochores were exposed to nocodazole, Mad2 rapidly reappeared at the kinetochores (Fig. 5 C). Together, these findings reveal that aurora B activity is not required for recruitment of Mad2 to kinetochores or for proper mitotic checkpoint function.

Mad2 also accumulates on kinetochores as Taxol (0.5–20 μM)-treated RPE1 (Fig. 4 E) and PtK2 (Fig. 5 D) cells enter mitosis in Hesperadin but, as for cells treated with Taxol only (Fig. 2, B and C), Mad2 is then progressively lost from all kinetochores after which the cells exit mitosis (Fig. 4, F and G; Fig. 5 D). Because the 90% reduction in the DM after inhibiting aurora B in Taxol-treated RPE1 cells is not due to a requirement for aurora B in the checkpoint (above), and because this accelerated exit does not occur in the presence of unattached (Mad2-positive) kinetochores, it must be due, as on monastrol spindles, to the depletion of free kinetochores via the stabilization of syntelic attachments (Fig. 4, F and G, arrowheads).

Elevated Taxol concentrations accelerate checkpoint satisfaction by stabilizing syntelic kinetochore attachments

In Taxol, progressive concentration increases stabilize MTs by inhibiting plus- and then minus-end MT dynamics in vitro (Derry et al., 1995, 1998) and in vivo (Jordan et al., 1993) until a point above which MT assembly is promoted. In HeLa, spindle MT mass begins to increase above 10 nM Taxol until it peaks at 330 nM, 500% above normal (Jordan et al., 1993). This is likely true for other cells, although the concentration for inducing maximum spindle MT mass may differ. Thus, in RPE1, checkpoint satisfaction may occur more rapidly in 5 vs. 0.5 μM Taxol because 5 μM promotes the formation of more MTs for recruitment by kinetochores. However, this cannot be the full story because in RPE1 increasing Taxol from 5 to 10 μM is unlikely to increase spindle MT mass, yet it decreases the DM from 5 to 3.5 h (Fig. 1).

As noted above, in Taxol the mitotic checkpoint cannot be satisfied until all kinetochores become stably attached to MTs, i.e., until existing monotelic and syntelic attachments are converted into amphitelic attachments or stable syntelic attachments. This being the case, an attractive explanation for why the DM is shorter in 5–10 μM versus 0.5 μM Taxol is that after a point, further concentration increases make it progressively more difficult for the error correction mechanism to produce free

kinetochores from syntelic attachments. To test this we asked if, in 500 nM Taxol, Mad2 can suddenly and transiently reappear on a kinetochore after it had lost its Mad2, as would occur during the correction and reformation of a syntelic attachment. We found that this does indeed occur in 0.5 μM Taxol (Fig. 2 B) and it leads to transient increases in the number of Mad2-positive kinetochores (Fig. 2 F). That this behavior was not seen in 20 μM Taxol (Fig. 2 G) implies that the correction mechanism is attenuated at elevated Taxol concentrations.

One prediction of our model is that inhibiting aurora B in Taxol-treated cells should, by stabilizing syntelic attachments, lead to a similar DM regardless of the drug concentration, and this too is the case: inhibiting aurora B in RPE1 treated with 0.5 or 10 μM Taxol decreases the DM from, respectively, 12 and 3.5 h to just 1.5 h (Table S1). Under these conditions, exit from mitosis coincides both with the depletion of YFP/Mad2 from the last Mad2-positive kinetochore (Fig. 5 D) and a sudden, rapid increase in the rate of cyclin B degradation (Fig. 3, C and D), i.e., from checkpoint satisfaction.

In summary, our results support a model in which Taxol delays cells in mitosis until the last monotelic chromosome establishes a normal amphitelic connection to an adjacent aster, which satisfies the mitotic checkpoint. As the Taxol concentration increases this event is progressively delayed due to the progressive inhibition of chromosome motion and MT dynamics. Then, at some point a concentration is reached in which further increases accelerate checkpoint satisfaction by making it more difficult to generate free (signaling) kinetochores from syntelic attachments formed in the drug. Although it is unclear how high Taxol concentrations stabilize syntelic attachments, it is noteworthy that as syntely is corrected the kinetochore that loses its MT attachment to a spindle pole (aster) remains oriented toward that pole because external forces are not present to move it to the opposite side of the centromere (Loncarek et al., 2007). Thus, even if the error correction mechanism breaks the MT attachments on a given kinetochore in >0.5 μM Taxol, e.g., by preventing Hec1 from binding MTs (DeLuca et al., 2006), the attachment should rapidly reform as the old Taxol-stabilized kinetochore fiber MTs are re-bound.

A reason why some cells are more sensitive to lower versus higher Taxol concentrations

We found that although 27% of RPE1 cells died in or shortly after mitosis in 0.5 μM Taxol (Brito and Rieder, 2009), only 1% died in 5–10 μM Taxol—and the same was true for epothilone B (Table S1). Similarly, Gascoigne and Taylor (2008) reported that almost all H1703 cells die during mitosis in 100 nM Taxol, whereas in 10 μM Taxol 63% escape as viable cells. In an earlier but more thorough study, Yeung et al. (1999) noted that after 24 h in 50 nM Taxol the mitotic index in four of six breast cancer lines ranged from 66–82%, and by 48 h 59–79% of the cells had died by apoptosis. However, after 24 h in 25 μM Taxol these same lines exhibited both a significantly lower mitotic index (6–15%) and a dramatic reduction (4–12%) in apoptosis. Thus, unlike for other spindle poisons some cells are, paradoxically, more sensitive to lower versus higher Taxol concentrations.

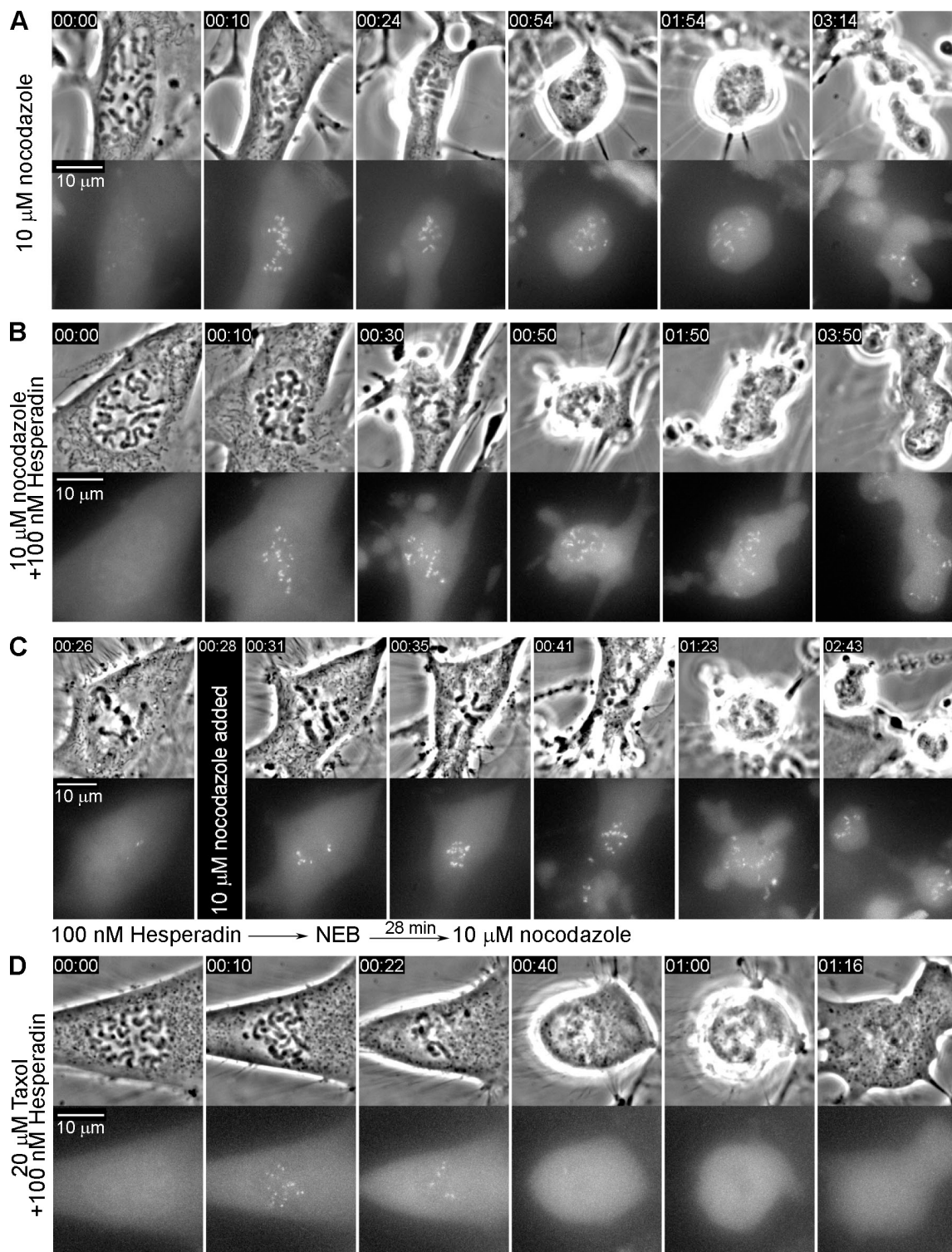


Figure 5. **Inhibiting aurora B with Hesperadin does not prevent Mad2 accumulation at kinetochores in nocodazole-treated Mad2/Plk2 cells.** (A and B) Mad2 rapidly reappears on kinetochores when Hesperadin-treated cells in metaphase are exposed to nocodazole (C). (D) By contrast, although Mad2 also accumulates at kinetochores as Taxol-treated cells enter mitosis in Hesperadin, it is depleted with time until all kinetochores lack Mad2 after which the cell exits mitosis (see also Fig. 2, C and D).

In general, the longer the mitotic checkpoint delays a cell in mitosis the more likely it is to die during or after mitosis. This implies that a “death switch” is thrown at some point during the prolonged mitosis after which the cell is destined to die (Rieder and Maiato, 2004; Tao et al., 2005). This being the case, our

finding that the DM in high Taxol concentrations is much shorter than in lower ones provides a potential explanation for the above paradox: for some cell types the delay in mitosis induced by 100–500 nM Taxol is long enough to trigger the death switch, whereas at higher concentrations the cells escape mitosis before this point.

Materials and methods

Cell culture

RPE1, BJ fibroblasts, HeLa, and U2OS were cultured in DME supplemented with 10% fetal bovine serum. PiK2 cells stably expressing Mad2-YFP were cultured in Ham's F12 medium (Invitrogen) supplemented with 10% fetal bovine serum. Cells were maintained at 37°C in a 5% CO₂ atmosphere and seeded onto coverslips 24–48 h before experimentation. All drugs were diluted in DMSO. Paclitaxel, vinblastine, and epothilone B were from Sigma-Aldrich, nocodazole and MG132 were from EMD.

Light microscopy

Immunostaining was as described previously (Brito et al., 2008). Rabbit anti-Mad2 antibody (a gift from E.D. Salmon, Chapel Hill, NC) was used at 1:400; human anti-centromere antibody (ACA) was used at 1:300 (Antibodies, Inc.); rat anti- α -tubulin antibody (YL1/2) was used at 1:5,000 (Novus Biologicals Inc.), and mouse anti-Hec1 (9g3.23) was used at 1:1,000 (Novus Biologicals, Inc.). DNA was stained with Hoechst 33342 (Invitrogen). Anti-human Alexa Fluor 488, anti-mouse Alexa Fluor 488, and anti-rabbit Alexa Fluor 546 (Invitrogen) were used at 1:500. Image stacks were acquired on a DeltaVision System (Applied Precision, LLC) centered on a microscope (model IX70; Olympus) and a camera (model CM350; Photometrics). Z-series image stacks were deblurred using the SoftWoRx 2.5 deconvolution algorithm (Applied Precision, LLC) and presented as maximal intensity projections.

For live cell imaging, coverslip cultures were mounted in Rose chambers and maintained at 37°C in phenol-free L-15 medium (Invitrogen) with 10% fetal bovine serum. For studies on the DM time-lapse phase-contrast images were acquired at 1–5-min intervals with a 20X (0.50 NA) PlanFluor objective mounted on an Eclipse TE 2000-U microscope (Nikon) or a 10X (0.25 NA) PlanFluor objective mounted on a DIAPHOT 200 microscope (Nikon). These microscopes were equipped with ORCA-ER cooled-CCD (Hamamatsu Photonics) or Micromax (Roper Scientific) cameras, and the imaging systems were driven by Image-Pro Plus 5.1 (Media Cybernetics, Inc.).

For studies on kinetochore-associated Mad2-YFP we used a 100 \times 1.4 NA PlanApo objective lens mounted on a microscope (model TE 2000-U; Nikon) equipped with a camera (Cascade 512B; Photometrics). Z-series image stacks were collected in both phase-contrast and YFP epifluorescence at 1- μ m steps throughout the depth of the cell. A narrow band-pass excitation filter was used to minimize the photobleaching. The cyclin B/GFP studies were conducted as detailed previously (Brito and Rieder, 2006; Brito et al., 2008). In brief, coverslip cultures of RPE1 cells were transfected with a cyclin B/GFP plasmid (a gift of Jon Pines, University of Cambridge, Cambridge, UK), after which they were returned to a 37°C incubator. 15 h later the coverslips were mounted in Rose chambers containing various concentrations of Taxol. These were then placed on the stage of a microscope (model TE2000E; Nikon) maintained at 37°C. Cyclin B/GFP-expressing prophase cells were located and followed into and through mitosis using a 40X 0.75 NA lens. Near-simultaneous phase-contrast and fluorescence images were acquired at 1–5-min intervals using a shuttered camera (Orca ER; Hamamatsu Photonics) as well as a narrow band-pass excitation filter for minimizing GFP photobleaching. Integrated fluorescence intensities were measured using ImageJ (National Institutes of Health, Bethesda, MD) and the method described by Hoffman et al. (2001). Surrounding interphase cells expressing cyclin B/GFP were used as photobleaching controls, and all intensities were normalized as the ratio to the first time-point image.

Statistics and quantization

Interkinetochore distances were measured only between sister kinetochore pairs on the spindle equator when both kinetochore dots were in the same optical section. Distance was defined as the space between the distal ends of the two ACA dots. Mad2 intensity was determined using the method of Hoffman et al. (2001). In brief, immunofluorescence image stacks were acquired using 300-nm steps on the DeltaVision System (Applied Precision, LLC) and the acquisition settings were the same for all samples. Because the distance between the sister kinetochores was too close to measure separately after depolymerizing MTs with nocodazole, sister kinetochores pairs were analyzed. The best in-focus image from a non-deconvolved z-series was chosen and only sister kinetochores in the same section (horizontal orientation) were selected for quantization. The intensity of Mad2 was normalized to the ACA level of the corresponding kinetochore pair, and 100 kinetochore pairs were examined from each of three separate experiments. The relative fluorescence intensity was obtained by converting the average intensity from nocodazole-treated cells to 1 and then

normalizing the value from cells treated with nocodazole plus Hesperadin accordingly. Integrated intensities were measured by ImageJ and the results were processed by Microsoft Excel software.

Online supplemental material

Table S1 summarizes how the duration of mitosis changes in RPE1, BJ fibroblasts, HeLa, and U2OS in response to various drug treatments. Fig. S1 documents the progressive depletion of Mad2 from kinetochores in Taxol-treated RPE1 cells when exit from mitosis is inhibited with MG132. Fig. S2 documents the lack of tension on centromeres in Taxol-treated RPE1 and PiK2 cells under conditions in which the mitotic checkpoint is satisfied. Online supplemental material is available at <http://www.jcb.org/cgi/content/full/jcb.200906150/DC1>.

We thank Dr. E.D. Salmon and members of his laboratory for supplying us with Mad2/YFP PiK2 cells and rabbit anti-Mad2 antibody.

This work was supported by National Institutes of Health GMS grant 40198 to C.L. Rieder.

Submitted: 23 June 2009

Accepted: 7 August 2009

References

- Ahonen, L.J., M.J. Kallio, J.R. Daum, M. Bolton, I.A. Manke, M.B. Yaffe, P.T. Stukenberg, and G.J. Gorbsky. 2005. Polo-like kinase 1 creates the tension-sensing 3F3/2 phosphoepitope and modulates the association of spindle-checkpoint proteins at kinetochores. *Curr. Biol.* 15:1078–1089.
- Brinkley, B.R., E. Stubblefield, and T.C. Hsu. 1967. The effects of colcemid inhibition and reversal on the fine structure of the mitotic apparatus of Chinese hamster cells in vitro. *J. Ultrastruct. Res.* 19:1–18.
- Brito, D.A., and C.L. Rieder. 2006. Mitotic checkpoint slippage in humans occurs via cyclin B destruction in the presence of an active checkpoint. *Curr. Biol.* 16:1194–1200.
- Brito, D.A., and C.L. Rieder. 2009. The ability to survive mitosis in the presence of microtubule poisons differs significantly between human nontransformed (RPE-1) and cancer (U2OS, HeLa) cells. *Cell Motil. Cytoskeleton.* 66:437–447.
- Brito, D.A., Z. Yang, and C.L. Rieder. 2008. Microtubules do not promote mitotic slippage when the spindle assembly checkpoint cannot be satisfied. *J. Cell Biol.* 182:623–629.
- Cai, S., C.B. O'Connell, A. Khodjakov, and C.E. Walczak. 2009. Chromosome congression in the absence of kinetochore fibres. *Nat. Cell Biol.* 11:832–838.
- Chang, D.C., N. Xu, and K.Q. Luo. 2003. Degradation of cyclin B is required for the onset of anaphase in mammalian cells. *J. Biol. Chem.* 278:37865–37873.
- Chen, R.-H., J.C. Waters, E.D. Salmon, and A.W. Murray. 1996. Association of spindle assembly checkpoint component XMAD2 with unattached kinetochores. *Science.* 274:242–246.
- Clute, P., and J. Pines. 1999. Temporal and spatial control of cyclin B1 destruction in metaphase. *Nat. Cell Biol.* 1:82–87.
- DeLuca, J.G., W.E. Gall, C. Ciferri, D. Cimino, A. Musacchio, and E.D. Salmon. 2006. Kinetochore microtubule dynamics and attachment stability are regulated by Hec1. *Cell.* 127:969–982.
- Derry, W.B., L. Wilson, and M.A. Jordan. 1995. Substoichiometric binding of taxol suppresses microtubule dynamics. *Biochemistry.* 34:2203–2211.
- Derry, W.B., L. Wilson, and M.A. Jordan. 1998. Low potency of taxol at microtubule minus ends: implications for its antimitotic and therapeutic mechanism. *Cancer Res.* 58:1177–1184.
- Ditchfield, C., V.L. Johnson, A. Tighe, R. Ellston, C. Haworth, T. Johnson, A. Mortlock, N. Keen, and S.S. Taylor. 2003. Aurora B couples chromosome alignment with anaphase by targeting BubR1, Mad2, and Cenp-E to kinetochores. *J. Cell Biol.* 161:267–280.
- Gascoigne, K.E., and S.S. Taylor. 2008. Cancer cells display profound intra- and interline variation following prolonged exposure to antimitotic drugs. *Cancer Cell.* 14:111–122.
- Hauf, S., R.W. Cole, S. LaTerra, C. Zimmer, G. Schnapp, R. Walter, A. Heckel, J. van Meel, C.L. Rieder, and J.-M. Peters. 2003. The small molecule Hesperadin reveals a role for Aurora B in correcting kinetochore-microtubule attachment and in maintaining the spindle assembly checkpoint. *J. Cell Biol.* 161:281–294.
- Hoffman, D.B., C.G. Pearson, T.J. Yen, B.J. Howell, and E.D. Salmon. 2001. MT dependent changes in the assembly of MT motor proteins and mitotic spindle checkpoint proteins at kinetochores. *Mol. Biol. Cell.* 12:1995–2009.
- Hornick, J.E., J.R. Bader, E.K. Tribble, K. Trimble, J.S. Breunig, E.S. Halpin, K.T. Vaughan, and E.H. Hinchliffe. 2008. Live-cell analysis of mitotic

- spindle formation in taxol-treated cells. *Cell Motil. Cytoskeleton*. 65:595–613.
- Iku, A.E., C.-P.H. Yang, T. Matsumoto, and S.B. Horwitz. 2005. Low concentrations of taxol cause mitotic delay followed by premature dissociation of p55CDC from Mad2 and BubR1 and abrogation of the spindle checkpoint, leading to aneuploidy. *Cell Cycle*. 4:1385–1388.
- Jordan, M.A., D.A. Thrower, and L. Wilson. 1992. Effects of vinblastine, podophyllotoxin and nocodazole on mitotic spindles. Implications for the role of microtubule dynamics in mitosis. *J. Cell Sci.* 102:401–416.
- Jordan, M.A., R.J. Toso, D.A. Thrower, and L. Wilson. 1993. Mechanism of mitotic block and inhibition of cell proliferation by taxol at low concentrations. *Proc. Natl. Acad. Sci. USA*. 90:9552–9556.
- Kapoor, T.M., T.U. Mayer, M.L. Coughlin, and T.J. Mitchison. 2000. Probing spindle assembly mechanisms with monastrol, a small molecule inhibitor of the mitotic kinesin, Eg5. *J. Cell Biol.* 150:975–988.
- Kapoor, T.M., M.A. Lampson, P. Hergert, L. Cameron, D. Cimini, E.D. Salmon, B.F. McEwen, and A. Khodjakov. 2006. Chromosomes can congress to the metaphase plate before biorientation. *Science*. 311:388–391.
- Lampson, M.A., K. Renduchitala, A. Khodjakov, and T.M. Kapoor. 2004. Correcting improper chromosome-spindle attachments during cell division. *Nat. Cell Biol.* 6:232–237.
- Lens, S.M.A., R.M.F. Wolthuis, R. Klompaker, J. Kauw, R. Agami, T. Brummelkamp, G. Kops, and R.H. Medema. 2003. Survivin is required for a sustained spindle checkpoint arrest in response to lack of tension. *EMBO J.* 22:2934–2947.
- Loncarek, J., O. Kisurina-Evgenieva, T. Vinogradova, P. Hergert, S. La Terra, T.M. Kapoor, and A. Khodjakov. 2007. The centromere geometry essential for keeping mitosis error free is controlled by spindle forces. *Nature*. 450:745–749.
- Maekawa, T., R. Leslie, and R. Kuriyama. 1991. Identification of a minus end-specific microtubule-associated protein located at the mitotic poles in cultured mammalian cells. *Eur. J. Cell Biol.* 54:255–267.
- Nicklas, R.B., J.C. Waters, E.D. Salmon, and S.C. Ward. 2001. Checkpoint signals in grasshopper meiosis are sensitive to microtubule attachment, but tension is still essential. *J. Cell Sci.* 114:4173–4183.
- O'Connell, C.B., J. Loncarek, P. Hergert, A. Kourtidis, D.S. Conklin, and A. Khodjakov. 2008. The spindle assembly checkpoint is satisfied in the absence of interkinetochore tension during mitosis with unreplicated genomes. *J. Cell Biol.* 183:29–36.
- Pinsky, B.A., C. Kung, K.M. Shokat, and S. Biggins. 2006. The Ipl1-Aurora protein kinase activates the spindle checkpoint by creating unattached kinetochores. *Nat. Cell Biol.* 8:78–83.
- Rieder, C.L., and H. Maiato. 2004. Stuck in division or passing through: what happens when cells cannot satisfy the spindle assembly checkpoint. *Dev. Cell*. 7:637–651.
- Ruchaud, S., M. Carmena, and W.C. Earnshaw. 2007. Chromosomal passengers: conducting cell division. *Nat. Rev. Mol. Cell Biol.* 8:798–812.
- Shi, J., J.D. Orth, and T. Mitchison. 2008. Cell type variation in responses to antimitotic drugs that target microtubules and kinesin-5. *Cancer Res.* 68:3269–3276.
- Skoufias, D.A., P.R. Andreassen, F.B. Lacroix, L. Wilson, and R.L. Margolis. 2001. Mammalian mad2 and bub1/bubR1 recognize distinct spindle-attachment and kinetochore-tension checkpoints. *Proc. Natl. Acad. Sci. USA*. 98:4492–4497.
- Skoufias, D.A., S. DeBonis, Y. Saoudi, L. Lebeau, I. Crevel, R. Cross, R.H. Wade, D. Hackney, and F. Kozielski. 2006. S-trityl-L-cysteine is a reversible, tight binding inhibitor of the human kinesin Eg5 that specifically blocks mitotic progression. *J. Biol. Chem.* 281:17559–17569.
- Sudo, T., M. Nitta, H. Saya, and N.T. Ueno. 2004. Dependence of paclitaxel sensitivity on a functional spindle assembly checkpoint. *Cancer Res.* 64:2502–2508.
- Tanaka, T.U., N. Rachidi, C. Janke, G. Pereira, M. Galova, E. Schiebel, M.J.R. Stark, and K. Nasmyth. 2002. Evidence that the Ipl1-Sli15 (Aurora kinase-INCENP) complex promotes chromosome bi-orientation by altering kinetochore-spindle pole connections. *Cell*. 108:317–329.
- Tao, W., V.J. South, Y. Zhang, J.P. Davide, L. Farrell, N.E. Kohl, L. Sepp-Lorenzino, and R.B. Lobell. 2005. Induction of apoptosis by an inhibitor of the mitotic kinesin KSP requires both activation of the spindle assembly checkpoint and mitotic slippage. *Cancer Cell*. 8:49–59.
- Uchida, K.S.K., K. Takagaki, K. Kumada, Y. Hirayama, T. Noda, and T. Hirota. 2009. Kinetochore stretching inactivates the spindle assembly checkpoint. *J. Cell Biol.* 184:383–390.
- Vader, G., C.W. Cuijzen, T. van Harn, M.J.M. Vromans, R.H. Medema, and S. M.A. Lens. 2007. The chromosomal passenger complex controls spindle checkpoint function independent from its role in correcting microtubule kinetochore interactions. *Mol. Biol. Cell*. 18:4553–4564.
- Waters, J.C., R.-H. Chen, A.W. Murray, and E.D. Salmon. 1998. Localization of Mad2 to kinetochores depends on microtubule attachment, not tension. *J. Cell Biol.* 141:1181–1191.
- Yeung, T.K., C. Germond, X. Chen, and Z. Wang. 1999. The mode of action of taxol: apoptosis at low concentration and necrosis at high concentration. *Biochem. Biophys. Res. Commun.* 263:398–404.

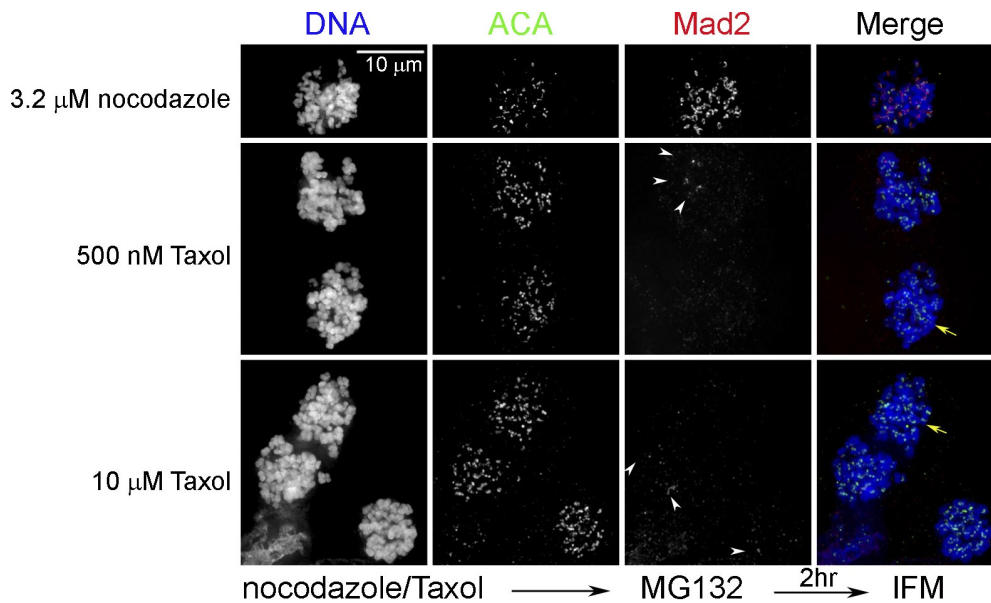
Yang et al., <http://www.jcb.org/cgi/content/full/jcb.200906150/DC1>

Figure S1. **In the presence of Taxol, Mad2 is progressively depleted from kinetochores in RPE1 cells.** Each row depicts mitotic RPE1 cell(s) in cultures that were exposed for 8–12 h to 3.2 μM nocodazole (top), 500 nM Taxol (middle) or 10 μM Taxol (bottom). During the last 2 h the cultures were exposed to 10 μM MG132 to prevent exit from mitosis, after which they were fixed and stained for centromeres (ACA) and Mad2. Note that one cell in the 500-nM and 10-μM panels (yellow arrows) entirely lack kinetochore-associated Mad2 staining. White arrowheads note kinetochore Mad2 staining.

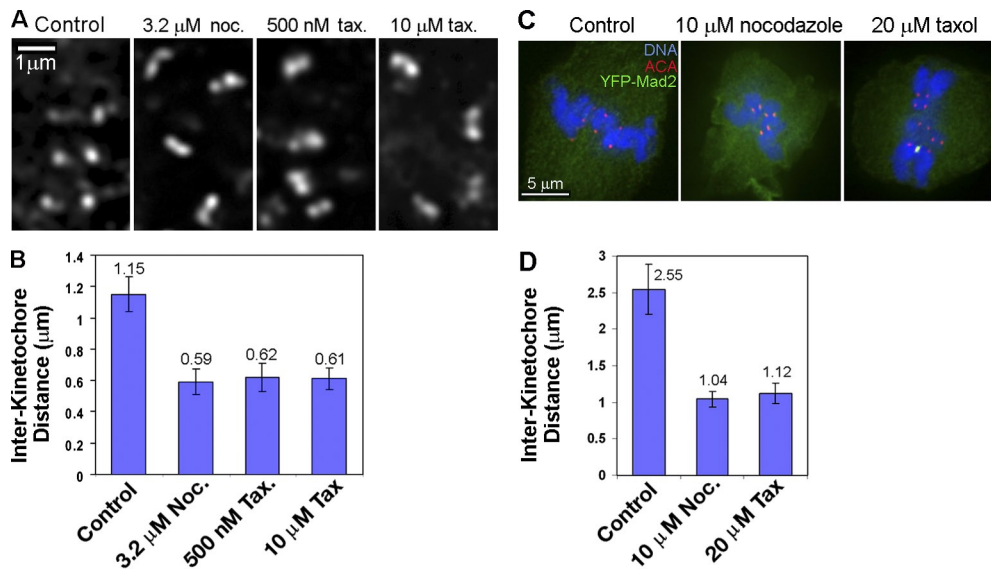


Figure S2. **Taxol-treated RPE1 and PtK2 cells satisfy the mitotic checkpoint in the absence of interkinetochore tension.** (A) The distance between sister kinetochores on ACA-stained centromeres was measured in nontreated metaphase cells, in nocodazole-treated cells lacking MTs, and in cells treated with 500 nM or 10 μM Taxol. (B) As for cells lacking MTs, there was no significant tension between sister kinetochores in either Taxol concentration. (C) Individual PtK2 cells were followed until they reached metaphase, after which they were either fixed (control) or treated for 5 min before fixation with 10 μM nocodazole or 20 μM Taxol. (D) Both nocodazole and Taxol rapidly eliminate the tension between sister kinetochores.

Table S1. The duration of mitosis (M) under various experimental conditions

Cell Type	Treatment	n	Duration of M	~ Duration of M	Survival
			min	h	
RPE1	None ^a	33	18 ± 3	0.3	100
	5-nM Taxol ^a	171	161 ± 85	2.5	99
	50-nM Taxol	132	510 ± 290	8.5	95
	500-nM Taxol ^a	112	729 ± 396	12	73
	5 μM Taxol	200	312 ± 165	5	99
	10 μM Taxol	200	224 ± 106	3.5	99
	5 nM Etoposilone B	193	154 ± 97	2.5	100
	500 nM Etoposilone B	70	800 ± 472	13	67
	2.5 μM Etoposilone B	158	263 ± 156	4.5	100
	3.2 μM nocodazole ^a	25	1140 ± 732	19	71
	3.2 μM nocodazole + 5 μM Taxol	158	564 ± 476	9	73
	10 μM vinblastine + 5 μM Taxol	35	1688 ± 405	28	23
	100 nM Hesperadin	108	20 ± 4	0.3	100
	3.2 μM nocodazole + 100 nM Hesperadin	66	1024 ± 228	17	
	500 nM Taxol + 100 nM Hesperadin	150	78 ± 26	1.3	100
10-μM Taxol + 100 nM Hesperadin	140	89 ± 29	1.5	100	
BJ	5 nM Taxol	110	165 ± 55	2.5	
	500 nM Taxol	106	1057 ± 459	18	
	5 μM Taxol	33	497 ± 333	8	
	10 μM Taxol	95	320 ± 224	5	
HeLa	5 nM Taxol	100	842 ± 321	14	
	500 nM Taxol	110	1483 ± 400	25	
	5 μM Taxol	80	997 ± 392	16.5	
U2OS	5 nM Taxol	120	63 ± 31	1	
	500 nM Taxol	132	591 ± 206	10	
	5 μM Taxol	120	483 ± 267	8	

All data are from ≥2 live-cell video records obtained on different days. The duration of M is as defined in Brito et al., 2008; n = number of cells.

^aFrom Brito et al., 2008.

References

Brito, D.A., Z. Yang, and C.L. Rieder. 2008. Microtubules do not promote mitotic slippage when the spindle assembly checkpoint cannot be satisfied. *J. Cell Biol.* 182:623–629.